

# Cysteine–Cystine Photoregeneration for Oxygenic Photosynthesis of Acetic Acid from CO<sub>2</sub> by a Tandem Inorganic–Biological Hybrid System

Kelsey K. Sakimoto,<sup>†,‡</sup> Stephanie J. Zhang,<sup>†</sup> and Peidong Yang<sup>\*,†,‡,§</sup>

<sup>†</sup>Department of Chemistry, University of California—Berkeley, Berkeley, California 94702, United States

<sup>‡</sup>Materials Sciences Division, Lawrence Berkeley National Laboratory, Berkeley, California 94702, United States

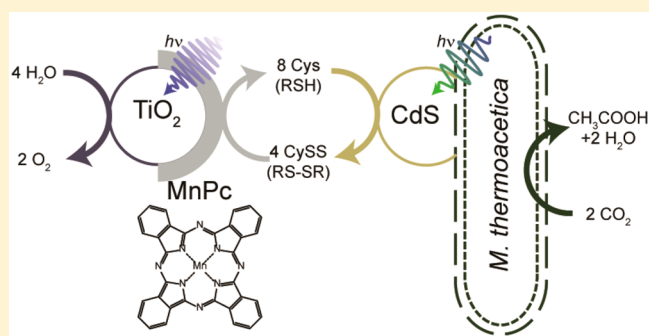
Department of Materials Science and Engineering, University of California—Berkeley, Berkeley, California 94702, United States

<sup>§</sup>Kavli Energy NanoSciences Institute, Berkeley, California 94702, United States

## Supporting Information

**ABSTRACT:** Tandem “Z-scheme” approaches to solar-to-chemical production afford the ability to independently develop and optimize reductive photocatalysts for CO<sub>2</sub> reduction to multicarbon compounds and oxidative photocatalysts for O<sub>2</sub> evolution. To connect the two redox processes, molecular redox shuttles, reminiscent of biological electron transfer, offer an additional level of facile chemical tunability that eliminates the need for solid-state semiconductor junction engineering. In this work, we report a tandem inorganic–biological hybrid system capable of oxygenic photosynthesis of acetic acid from CO<sub>2</sub>. The photoreductive catalyst consists of the bacterium *Moorella thermoacetica* self-photosensitized with CdS nanoparticles at the expense of the thiol amino acid cysteine (Cys) oxidation to the disulfide form cystine (CySS). To regenerate the CySS/Cys redox shuttle, the photooxidative catalyst, TiO<sub>2</sub> loaded with cocatalyst Mn(II) phthalocyanine (MnPc), couples water oxidation to CySS reduction. The combined system *M. thermoacetica*–CdS + TiO<sub>2</sub>–MnPc demonstrates a potential biomimetic approach to complete oxygenic solar-to-chemical production.

**KEYWORDS:** Cadmium sulfide, titanium dioxide, *Moorella thermoacetica*, phthalocyanine, solar-to-chemical production, artificial photosynthesis



Though they may project to outcompete natural photosynthesis, the conversion of solar energy into chemical bonds remains a daunting task for current artificial systems.<sup>1</sup> Many semiconductor light harvesters have been developed as both monolithic photoelectrodes and suspended nanoparticle photocatalysts.<sup>2</sup> However, the development of cheap, efficient, and selective cocatalysts remains challenging for water oxidation and particularly for CO<sub>2</sub> reduction to multicarbon compounds.<sup>3</sup> Biomimetic cocatalysts that emulate the active sites of the proteins employed within natural photosynthesis have yet to fully capture the performance of their biological inspiration due to the inherent complexity of enzyme catalysis.<sup>4</sup>

To skirt these difficulties, several studies have recently demonstrated the use of whole cells and whole protein complexes in solar-to-chemical production schemes.<sup>5–9</sup> We have recently shown the ability of the acetogenic bacterium *Moorella thermoacetica* to self-photosensitize by bioprecipitation of CdS nanoparticles, facilitating photosynthesis of acetic acid from CO<sub>2</sub>.<sup>10</sup> While this system demonstrates high-efficiency photoreductive capabilities, the inorganic–biological hybrid organism operates at the expense of a sacrificial reductant, the

thiol amino acid cysteine (Cys), which oxidizes to the disulfide form, cystine (CySS).

Direct photooxidation of water to O<sub>2</sub> by *M. thermoacetica*–CdS is infeasible due to the poor oxidative stability of many metal chalcogenides.<sup>11</sup> We have thus taken a biomimetic approach based on the tandem “Z-scheme” design, in which photoreduction and photooxidation are carried out by two separate light harvesters and cocatalysts.<sup>12</sup> To balance the CO<sub>2</sub> photoreduction of *M. thermoacetica*–CdS, TiO<sub>2</sub> nanoparticles were selected due to their well-characterized performance as water oxidation photocatalysts as well as their high stability.<sup>13</sup>

Within tandem systems, two choices for linking photoreduction and photooxidation exist: (1) a direct solid-state junction and (2) a redox mediator. Though direct contact between the two semiconductor light absorbers could afford fast electrical conduction, optimization and engineering of the junction remain nontrivial due to the formation of detrimental

Received: July 3, 2016

Revised: August 10, 2016

Published: August 18, 2016

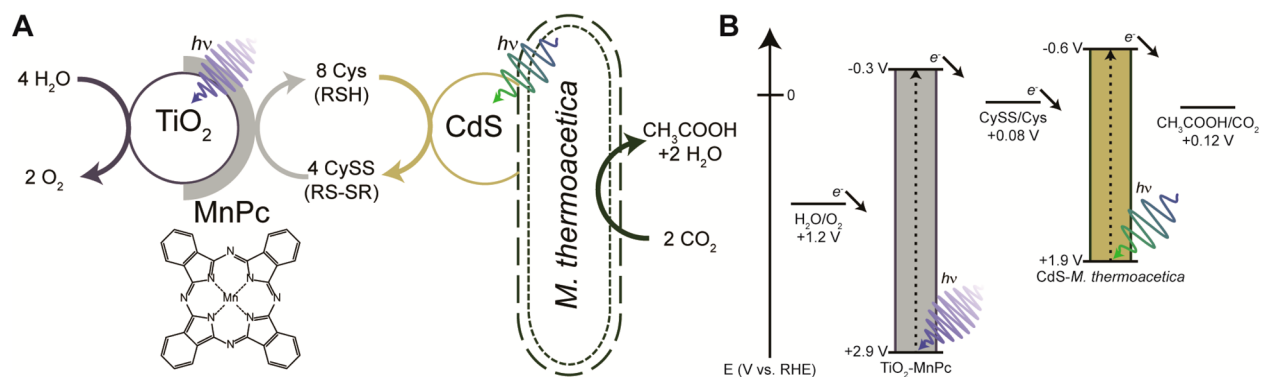


**Figure 1.** Schematic of the *M. thermoacetica*–CdS + TiO<sub>2</sub>–MnPc tandem system. (A) Illumination of *M. thermoacetica*–CdS drives the reduction of CO<sub>2</sub> into acetic acid, coupled to the oxidation of Cys to CySS. Co-illumination of TiO<sub>2</sub>–MnPc drives the reduction of CySS back into Cys, coupled to oxidation of water to H<sub>2</sub>O. (B) Energy level diagram depicting the relative alignment of the TiO<sub>2</sub> and CdS with the relevant redox reactions.

charge transfer barriers.<sup>14</sup> The junctions that form are highly dependent on the material, band structure, and doping of the semiconductor, rendering this approach nongeneral, thus requiring reoptimization with the discovery of new and better semiconductor light absorbers. Additionally, close proximity between oxidative and reductive processes may lead to significant back reactions at the opposing semiconductor resulting in net loss in photosynthetic products.<sup>15</sup> In contrast, molecular redox mediators, which are widely employed within natural photosynthesis, afford a more facile connection to biological catalysts and offer a wide range of tunability via molecular synthetic chemistry as opposed to solid-state chemistry.

Taking inspiration from biological redox processes, a biocompatible CySS/Cys redox couple (RSH/RSSR) was selected.<sup>16</sup> As depicted in Figure 1, the tandem system investigated here consists of a TiO<sub>2</sub> nanoparticle loaded with a manganese(II) phthalocyanine (MnPc) cocatalyst to reduce CySS back into Cys, rendering the formerly sacrificial reductant into a regenerative redox couple.

The choice of a selective CySS reduction cocatalyst was crucial to prevent degradation of the CySS/Cys redox couple. Bare TiO<sub>2</sub> alone has been shown to be a poor photocatalyst for CySS reduction due to irreversible degradation.<sup>17,18</sup> Additionally, the inability of TiO<sub>2</sub> to absorb visible light severely limits its performance under solar illumination. Previous studies have reported on the electrochemical selectivity of various transition metal phthalocyanines (TMPc) to CySS reduction and Cys oxidation and have suggested that MnPc displays the highest activity toward CySS reduction of the first row transition metals due to its stronger binding of Mn to CySS.<sup>19</sup> Several first row TMPcs and unmetallated H<sub>2</sub>Pc were tested under in vitro conditions suitable for *M. thermoacetica*–CdS photosynthesis by loading on to TiO<sub>2</sub> nanoparticles and measuring Cys production rate under illumination (5% sun, AM1.5G). Reflectance spectra of the TiO<sub>2</sub>–TMPc photocatalysts were taken to confirm loading of MnPc (Figure 2) and display strong retention of the absorption peaks of the molecular cocatalyst.

As presented in Table 1, MnPc exhibited the highest activity for CySS reduction. The time series presented in Figure 3 under an inert N<sub>2</sub> atmosphere as well 21% O<sub>2</sub> demonstrate that, even in the presence of an oxidant, photocatalyst illumination results in net Cys production and a steady state Cys concentration. However, the rate of CySS reduction eventually plateaus as the rate of oxidation back into CySS matches that of

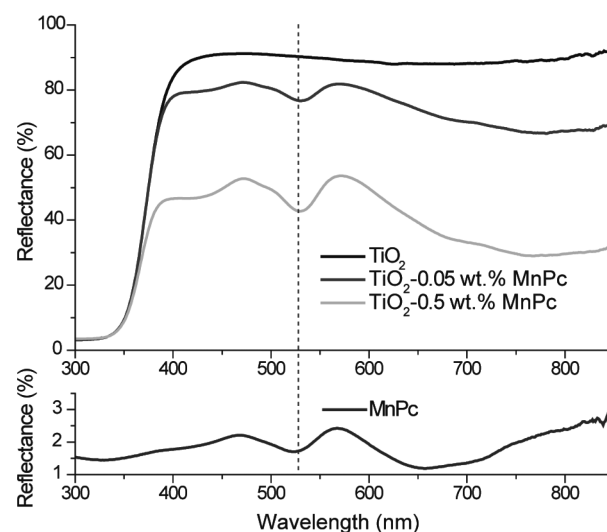


**Figure 2.** Reflectance spectra of TiO<sub>2</sub>–MnPc. Successful loading of increasing amounts of MnPc loaded onto TiO<sub>2</sub> as evidenced by sub-400 nm absorption. While the position of the peak at 530 nm remains consistent between the discrete and loaded MnPc, the lower energy peaks at ~650 nm broaden and red-shift once loaded onto TiO<sub>2</sub>.

**Table 1.** CySS Reduction Rate of Phthalocyanine Loaded TiO<sub>2</sub> Photocatalysts

| catalyst                       | rate ( $\mu\text{M Cys h}^{-1}$ ) |
|--------------------------------|-----------------------------------|
| no catalyst                    | 53.0 $\pm$ 9.3                    |
| MnPc (0.1 wt %) <sup>a</sup>   | 65.9 $\pm$ 4.6                    |
| MnPc (0.05 wt %) <sup>a</sup>  | 130.1 $\pm$ 8.4                   |
| MnPc (0.01 wt %) <sup>a</sup>  | 75.9 $\pm$ 3.3                    |
| FePc <sup>b</sup>              | 61.9 $\pm$ 4.5                    |
| CoPc <sup>b</sup>              | 56.4 $\pm$ 2.2                    |
| NiPc <sup>b</sup>              | 87.7 $\pm$ 18.7                   |
| CuPc <sup>b</sup>              | 68.7 $\pm$ 5.8                    |
| ZnPc <sup>b</sup>              | 45.2 $\pm$ 5.7                    |
| H <sub>2</sub> Pc <sup>b</sup> | 75.5 $\pm$ 12.8                   |

<sup>a</sup>Catalyst loading relative to mass of TiO<sub>2</sub>. <sup>b</sup>Equimolar to 0.05 wt % MnPc. The standard deviation represents error associated with linear regression of kinetic data.

the forward reaction. However, this insight demonstrates that the TiO<sub>2</sub>–MnPc photocatalyst system is compatible with aerobic conditions and net O<sub>2</sub> production.

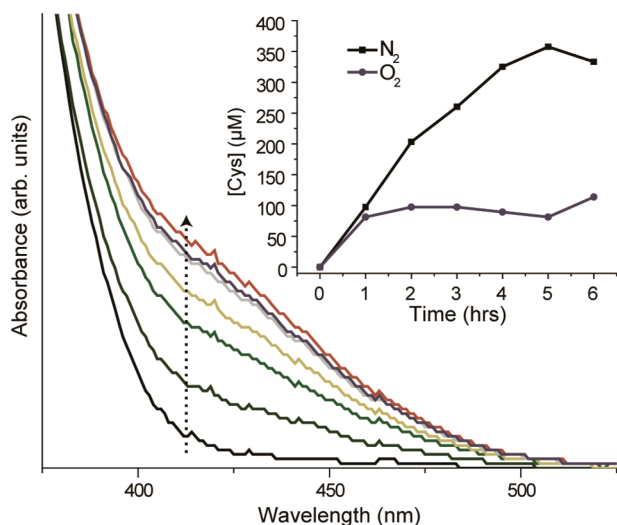


**Figure 3.** CySS photoreduction kinetics of  $\text{TiO}_2\text{-MnPc}$ . A colorimetric assay employing Ellman's reagent monitored the progress of Cys photogeneration. (inset)  $\text{TiO}_2\text{-MnPc}$  demonstrated net CySS photoreduction under both anaerobic and aerobic conditions.

The nonlinear trend of CySS reduction activity with increasing an number of  $d$ -electrons deviates from the monotonic decreasing trend observed in previous reports.<sup>19</sup> Specifically, we observe a local peak in activity for NiPc and CuPc which have exhibited the poorest dark electrochemical activity. In addition, MnPc displays a significantly higher activity than all other tested Pc. While previous electrochemical studies employed relatively inert and noninteracting graphitic electrodes, reflectance spectra (Figure 2, S1) demonstrate a redshift in the low energy peaks around 650 nm, suggesting coupling between  $\text{TiO}_2$  and MnPc. The solubility of TMPc in EtOH (the solvent used for loading) may play a role, as MnPc has the highest EtOH solubility, perhaps leading to more even loading on  $\text{TiO}_2$  and a greater number of exposed active sites.<sup>20</sup> However, both NiPc and CuPc have demonstrated lower

solubility than FePc and CoPc, indicating that differences in cocatalyst loading fails to sufficiently explain the activity trend.

The spectrum of  $\text{TiO}_2\text{-MnPc}$  retains the distinct peak at 530 nm found in the neat MnPc spectrum (Figure 2), whereas such spectral signatures are often lost in the other  $\text{TiO}_2\text{-Pc}$  photocatalysts, suggesting either poor loading or perhaps interactions between the TMPc and  $\text{TiO}_2$  (Figure S1). However, activity does not directly correlate with reflectance spectra, as NiPc and ZnPc which show the second highest and lowest activity, respectively, have similar reflectance spectra with deemphasized features.

Since previous studies were conducted as electrocatalysts in dark, the differences in activity observed here suggest TMPc visible light absorption has an effect on catalytic performance. TMPcs have been widely employed as visible and IR sensitizers of dye-sensitized solar cells (DSSCs) due to the favorable energy alignment of their HOMO and LUMO with the conduction band of  $\text{TiO}_2$ .<sup>21</sup> We do note that ZnPc, a common visible light sensitizer in DSSCs, demonstrates the lowest activity, perhaps due to the favorable charge injection from ZnPc to  $\text{TiO}_2$  that would impede CySS reduction.

The activity of NiPc deviates most drastically from previous reports. While Zagal et al. report NiPc as one of the least catalytically active for CySS reduction, photocatalytically, NiPc was the second most active behind MnPc. Analysis of the MO diagram of NiPc shows that the HOMO-LUMO charge transfer is a ligand-to-metal charge transfer (LMCT) from the Pc  $a_{1u}$  to the Ni  $3d_{x^2-y^2}$  centered  $b_{1g}$ .<sup>22</sup> This shift of electron density toward the metal active site under illumination may improve CySS binding and increase reduction activity. In contrast, FePc and CoPc, the least photocatalytically active, exhibit largely metal-to-ligand charge transfer (MLCT) which may disfavor CySS binding. A similar LMCT argument may explain the higher activity of CuPc.  $\text{H}_2\text{Pc}$  also demonstrates reasonable activity toward CySS reduction despite not having a metal site to facilitate disulfide binding. However, the close proximity of two hydrogens may favor a proton-coupled electron transfer.

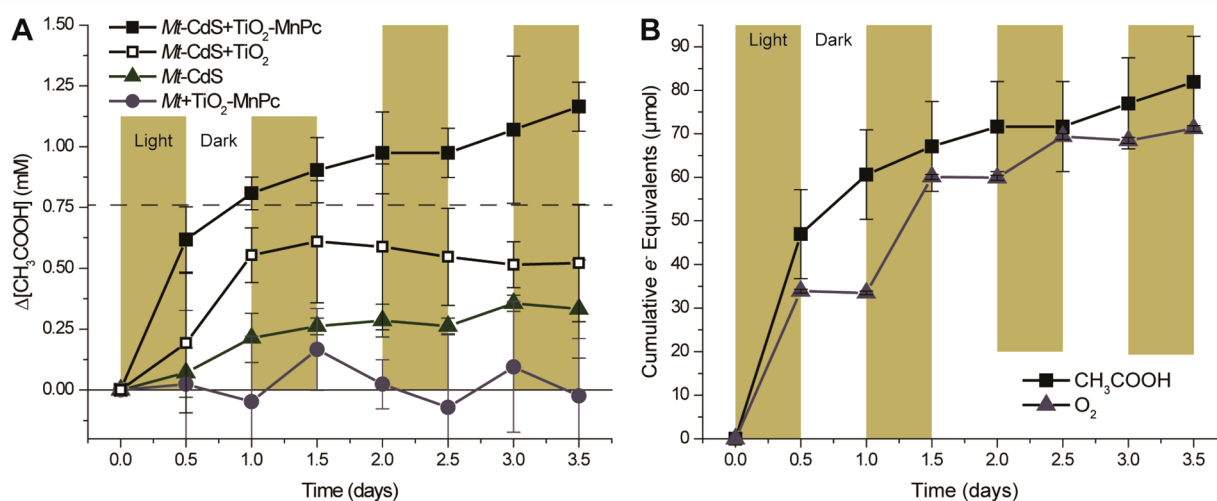


**Figure 4.** Photosynthetic performance of *M. thermoacetica*-CdS and  $\text{TiO}_2\text{-MnPc}$  tandem system. (A) Comparison of *M. thermoacetica*-CdS and  $\text{TiO}_2\text{-MnPc}$  with controls show greater acetic acid production from the combination of the tandem system. Both *M. thermoacetica*-CdS only and *M. thermoacetica* +  $\text{TiO}_2\text{-MnPc}$  controls showed lower acetic acid production below the stoichiometric limit imposed by Cys (dashed line). Without MnPc, the tandem system with bare  $\text{TiO}_2$  performs poorer. (B) Comparison of acetic acid ( $8e^-$ ) and  $\text{O}_2$  ( $4e^-$ ) cumulative electron equivalents measured over the course of 3.5 days showing strong correlation between reduced (acetic acid) and oxidized products ( $\text{O}_2$ ). All values represent the average and standard deviation of triplicate experiments.

Illumination of various combinations of *M. thermoacetica*–CdS and TiO<sub>2</sub>–MnPc demonstrated that the CySS photo-regenerative catalyst effectively pairs with the CO<sub>2</sub> photo-reductive catalyst (Figure 4). When only *M. thermoacetica*–CdS was illuminated, the rate of acetic acid production leveled off after roughly 1 day, below the stoichiometric limit set by Cys as limiting reagent (i.e., no photoregeneration). This rate is suboptimal, in part, due to the high photon flux, which lowers the efficiency of photosynthesis compared to previous low light illumination schemes. However, it enables a fair comparison to TiO<sub>2</sub> paired systems which require high photon fluxes. Similarly, combination of TiO<sub>2</sub>–MnPc with CdS-free *M. thermoacetica* cells yielded negligible acetate production (Figure 4A). While the band gap of TiO<sub>2</sub> is thermodynamically sufficient to drive microbially catalyzed CO<sub>2</sub> reduction, the process remains kinetically unfavorable due to the poor interface between TiO<sub>2</sub>–MnPc and *M. thermoacetica*. TiO<sub>2</sub> may also photosterilize *M. thermoacetica* in the absence of CdS nanoparticles via the formation of reactive oxygen species (ROS).<sup>23</sup> Finally, the combination of *M. thermoacetica*–CdS for CO<sub>2</sub> reduction to acetic acid and Cys oxidation, coupled with TiO<sub>2</sub>–MnPc for CySS reduction and water oxidation produced a net amount of acetic acid at a higher rate than *M. thermoacetica*–CdS alone, and above the stoichiometric limit of Cys, clear evidence of CySS/Cys as a regenerative redox couple. The photoprotective role of TiO<sub>2</sub> (in addition to the protection afforded by CdS alone) may also help to explain the higher photosynthetic rate of *M. thermoacetica* + TiO<sub>2</sub>–MnPc compared to *M. thermoacetica*–CdS alone.<sup>24</sup> The combination of *M. thermoacetica*–CdS + bare TiO<sub>2</sub> yielded more acetic acid than *M. thermoacetica*–CdS alone, but less than that of TiO<sub>2</sub>–MnPc, demonstrating the catalytic action of MnPc for selective CySS reduction, leading to a more effective regenerative redox couple and longer sustained acetic acid photosynthesis. Comparison of electron yields for the reduced product (acetic acid) and oxidative products (O<sub>2</sub>) shows comparable stoichiometries (Figure 4B). As expected, no O<sub>2</sub> is produced in the absence of light. However, dark acetic acid production is observed as is consistent with previous reports.<sup>10</sup> The oxidative electron yield (as O<sub>2</sub>) is slightly lower than the reductive products, potentially due to the net oxidation of some Cys.

While the current system demonstrates reasonable net kinetic performance, several improvements could be made to further increase the photosynthetic rate. As seen in both Figure 3 (inset) and Figure 4A, the rate of CySS reduction or acetic acid production begins to decrease from the initial rate, likely due to the effects of O<sub>2</sub> accumulation. As the partial pressure of O<sub>2</sub> rises, the back reaction of Cys oxidation begins to compete, giving a steady state concentration of Cys below the ~6 mM desired for high CO<sub>2</sub> reduction rates by *M. thermoacetica*–CdS. Additionally, the O<sub>2</sub> sensitivity of CdS and the anaerobic *M. thermoacetica* likely limit their performance at higher O<sub>2</sub> concentrations.<sup>25</sup> While engineering approaches such as gas purging could limit the detrimental effects of O<sub>2</sub>, a more elegant solution would call for physically separating the two incompatible processes through either physical space, or via a selective membrane.<sup>26</sup> While physically separating the oxidative and reductive photocatalysts would create significant difficulties for solid-junction nanoparticle tandem systems, the use of a molecular redox shuttle enabled by diffusional or convective transport renders this design readily accessible.

The limited light absorption of TiO<sub>2</sub> and CdS likely bottlenecks the solar-to-chemical efficiency of the current

system. Exploration of the semiconductor parameters space may yield lower bandgap semiconductors to raise the theoretical limit on solar-conversion efficiency. Due to the relative ease of engineering molecular rather than solid-state interfaces, the various components of this modular tandem inorganic–biological hybrid system may be switched out as newer, better performing materials become available. With these advances, this paradigm holds promise for the future of advanced solar-to-chemical production.

## ■ ASSOCIATED CONTENT

### 📄 Supporting Information

The Supporting Information is available free of charge on the ACS Publications website at DOI: 10.1021/acs.nanolett.6b02740.

Figures S1–2 and materials and methods (PDF)

## ■ AUTHOR INFORMATION

### Corresponding Author

\*E-mail: p\_yang@berkeley.edu.

### Notes

The authors declare no competing financial interest.

## ■ ACKNOWLEDGMENTS

K.K.S. acknowledges support from the NSF Graduate Research Fellowship Program under grant DGE-1106400. Solar-to-chemical production experiments were supported by the NSF under grant DMR-1507914. The authors thank J. J. Gallagher and M. C. Y. Chang for the original inoculum of *M. thermoacetica* ATCC 39073.

## ■ REFERENCES

- (1) Kim, D.; Sakimoto, K. K.; Hong, D.; Yang, P. *Angew. Chem., Int. Ed.* **2015**, *54* (11), 3259–3266.
- (2) Osterloh, F. E. *Chem. Soc. Rev.* **2013**, *42* (6), 2294–2320.
- (3) Kumar, B.; Llorente, M.; Froehlich, J.; Dang, T.; Sathrum, A.; Kubiak, C. P. *Annu. Rev. Phys. Chem.* **2012**, *63*, 541–569.
- (4) Magnuson, A.; Anderlund, M.; Johansson, O.; Lindblad, P.; Lomoth, R.; Polivka, T.; Ott, S.; Stensjö, K.; Styring, S.; Sundström, V.; Hammarström, L. *Acc. Chem. Res.* **2009**, *42* (12), 1899–1909.
- (5) Torella, J. P.; Gagliardi, C. J.; Chen, J. S.; Bediako, D. K.; Colón, B.; Way, J. C.; Silver, P. A.; Nocera, D. G. *Proc. Natl. Acad. Sci. U. S. A.* **2015**, *112* (8), 2337–2342.
- (6) Liu, C.; Gallagher, J. J.; Sakimoto, K. K.; Nichols, E. M.; Chang, C. J.; Chang, M. C. Y.; Yang, P.; Christopher, J. *Nano Lett.* **2015**, *15* (5), 3634–3639.
- (7) Nichols, E. M.; Gallagher, J. J.; Liu, C.; Su, Y.; Resasco, J.; Yu, Y.; Sun, Y.; Yang, P.; Chang, M. C. Y.; Chang, C. J. *Proc. Natl. Acad. Sci. U. S. A.* **2015**, *112* (37), 11461–11466.
- (8) Wang, W.; Chen, J.; Li, C.; Tian, W. *Nat. Commun.* **2014**, *5*, 4647.
- (9) Liu, C.; Colon, B. C.; Ziesack, M.; Silver, P. A.; Nocera, D. G. *Science (Washington, DC, U. S.)* **2016**, *352* (6290), 1210–1213.
- (10) Sakimoto, K. K.; Wong, A. B.; Yang, P. *Science (Washington, DC, U. S.)* **2016**, *351* (6268), 1–17.
- (11) Meissner, D.; Memming, R. *J. Phys. Chem.* **1988**, *92*, 3476–3483.
- (12) Kudo, A.; Miseki, Y. *Chem. Soc. Rev.* **2009**, *38* (1), 253–278.
- (13) Chen, X.; Mao, S. S. *Chem. Rev.* **2007**, *107* (7), 2891–2959.
- (14) Resasco, J.; Zhang, H.; Kornienko, N.; Becknell, N.; Lee, H.; Guo, J.; Brisenno, A. L.; Yang, P. *ACS Cent. Sci.* **2016**, *2*, 80.
- (15) Liu, C.; Tang, J.; Chen, H. M.; Liu, B.; Yang, P. *Nano Lett.* **2013**, *13* (6), 2989–2992.
- (16) Paulsen, C. E.; Carroll, K. S. *Chem. Rev.* **2013**, *113* (7), 4633–4679.

- (17) Nosaka, A. Y.; Tanaka, G.; Nosaka, Y. *J. Phys. Chem. B* **2012**, *116*, 11098–11102.
- (18) Machado, A. E. H.; França, M. D.; Velani, V.; Magnino, G. A.; Velani, H. M. M.; Freitas, F. S.; Müller, P. S.; Sattler, C.; Schmücker, M. *Int. J. Photoenergy* **2008**, *2008*, 482373.
- (19) Zagal, J. H.; Herrera, P. *Electrochim. Acta* **1985**, *30* (4), 449–454.
- (20) Ghani, F.; Kristen, J.; Riegler, H. *J. Chem. Eng. Data* **2012**, *57*, 439–449.
- (21) Giribabu, L.; Vijay Kumar, C.; Gopal Reddy, V.; Yella Reddy, P.; Srinivasa Rao, C.; Jang, S. R.; Yum, J. H.; Nazeeruddin, M. K.; Grätzel, M. *Sol. Energy Mater. Sol. Cells* **2007**, *91* (17), 1611–1617.
- (22) Liao, M. S.; Scheiner, S. *J. Chem. Phys.* **2001**, *114* (22), 9780–9791.
- (23) Ireland, J. C.; Klostermann, P.; Rice, E. W.; Clark, R. *Appl. Environ. Microbiol.* **1993**, *59* (5), 1668–1670.
- (24) Holmes, J. D.; Smith, P. R.; Evans-Gowing, R.; Richardson, D. J.; Russell, D. A.; Sodeau, J. R. *Photochem. Photobiol.* **1995**, *62* (6), 1022–1026.
- (25) Karnholz, A.; Küsel, K.; Gößner, A.; Drake, H. L.; Schramm, A. *Appl. Environ. Microbiol.* **2002**, *68* (2), 1005.
- (26) Giddings, C. G. S.; Nevin, K. P.; Woodward, T.; Lovley, D. R.; Butler, C. S. *Front. Microbiol.* **2015**, *6*, 1–6.